



## Photocatalytic removal of endocrine disrupting compounds from aqueous solution by different size nano-TiO<sub>2</sub> under artificial UVA

Emine Basturk<sup>a,b,\*</sup>, Mustafa Karatas<sup>a</sup>

<sup>a</sup>Department of Environmental Engineering, Faculty of Engineering, Aksaray University, 68100 Aksaray, Turkey, Tel. +90 382 288 3601; emails: eminebasturk@hotmail.com (E. Basturk), mkaratas33@gmail.com (M. Karatas)

<sup>b</sup>Department of Environmental Protection Technologies, Technical Sciences Vocational School, Aksaray University, 68100 Aksaray, Turkey

Received 9 October 2020; Accepted 20 February 2021

---

### ABSTRACT

In the present study, titanium dioxide (TiO<sub>2</sub>) nano-photocatalyst was characterized and used for the removal of estrone (E1) and estriol (E3), which are endocrine disrupting compounds (EDCs). The photocatalytic process is a very interesting alternative for the removal of such EDCs that is identified on the watch list of EU Decision 2015/495. The effects of operating parameters such as pH (3–10), contact time (1–10 min) and catalyst dose (0.025–0.100 g) were investigated. It was revealed that nano-TiO<sub>2</sub> exhibited a significantly enhanced photocatalytic efficiency toward E1 and E3 degradation. The increased efficiency was attributed to increased catalyst dosage, decreased pH value and smaller catalyst size. In general, it was observed that the presence of TiO<sub>2</sub> enhanced the photodegradation of E1 and E3; and that the particle size of TiO<sub>2</sub> was an important factor influencing dye removal. In the kinetic study, our study is fitted by Langmuir–Hinshelwood model. In addition, the humic acid and co-existing anion concentrations were also investigated.

*Keywords:* Endocrine disrupting compound; Estriol; Estrone; Nano-titanium dioxide; Photocatalytic degradation; Watch list of EU Decision 2015/495

---

### 1. Introduction

Several contaminants of emerging concern (CECs) can be natural or anthropogenic substances found at concentrations between ng/L and µg/L levels have a negative impact on aquatic compartments, such as surface water, groundwater and even drinking water, and include pesticides, industrial compounds, pharmaceuticals, personal care products, steroid hormones, drugs of abuse and others [1,2]. These CECs consumed by both humans and animals are not completely assimilated, but instead, they are excreted unchanged or as metabolites, back into the aquatic environment [3]. Endocrine disrupting compounds (EDCs) which are leading to increased global awareness and concern are one of the most important categories of emerging contaminants that pose a serious threat to not only aquatic

organisms but also terrestrial health [4]. Various processes have been designed to produce high-quality drinking water through the removal of these pollutants from surface waters [5]. Advanced oxidation processes, such as the Fenton process [6], ozonation [7], photocatalysis [8], photocatalytic degradation [9] and direct photolysis [10] have been investigated for steroid hormone removal. Most pharmaceuticals are recalcitrant to oxidation and are not easily decomposed. In recent years, ultraviolet (UV) irradiation has been proposed to be effective for oxidation [11]. Photocatalysis follows a series of basic steps that occur inside the irradiated catalyst (e.g., charge carrier production) and also on the surface where interfacial redox reactions subsequently produce reactive species (free electron e<sup>-</sup> and electron-hole h<sup>+</sup>) that oxidize refractory organic pollutants that are at or near the surface in the presence of solid catalyst

---

\* Corresponding author.

such as nano-titanium dioxide ( $\text{TiO}_2$ ) has been receiving more attention in water treatment studies due to the nonspecific nature of reactive oxygen species produced under UV irradiation [12–14].

The main aim of the present study was to use highly active  $\text{TiO}_2$  nanoparticles that have different particle dimensions. The photocatalytic removal of estrone (E1) in aqueous  $\text{TiO}_2$  dispersions and UV irradiation as well as the dependence of photo-oxidation rate on the parameters of (i)  $\text{TiO}_2$  (10 nm) and  $\text{TiO}_2$  (10–25 nm), (ii) catalyst amount, (iii) pH effect and (iv) kinetic study was also investigated.

## 2. Materials and methods

### 2.1. Materials

The  $\text{TiO}_2$  anatase (anatase >99%, crystalline size 10 nm and 10–25 nm) was purchased from Ege Nanotek Chemical, Turkey. For the preliminary experiments, the certificated reference material (CRM) materials, steroids and pharmaceuticals mix were obtained from Restek. The estrogen hormones (Estrone (CAS 53-16-7), Estriol (CAS 50-27-1)) were purchased from Sigma-Aldrich and Dr. Ehrenstorfer GmbH and also acetonitrile, NaOH,  $\text{H}_2\text{SO}_4$ , pyridine, and derivatization reagents (N,O-bis(trimethylsilyl)trifluoroacetamide (BSTFA) and 1% trimethylchlorosilane (TMCS)) were obtained from Sigma-Aldrich. All of the chemicals were used as received without any further purification. All of the solutions were prepared using ultrapure water from a Milli-Q synthesis unit (Millipore). The physical and chemical properties of the  $\text{TiO}_2$  (anatase) are given in Table 1.

### 2.2. Catalyst characterization

The X-ray diffraction (XRD) measurements of the samples were carried out with an X-ray diffractometer (Bruker D8 Advance X-ray Diffractometer) operating with a Cu K radiation wavelength of 1.54059 Å at room temperature. Data were collected over 2 h values from 200 to 880 at a speed of 20/min to assess the crystallinity and confirm the structure and phase. The pH at the point of zero charge ( $\text{pH}_{\text{pzc}}$ ) for the catalyst was determined using the batch equilibration technique.

### 2.3. Analyses and experimental procedure

The analytical procedure was carried out according to the EPA 1698 method. All of the samples were prepared before measuring to GC/MS by liquid–liquid extraction.

Table 1  
Anatase  $\text{TiO}_2$  properties

Purity	99%
Average particle dimension	10 nm
Surface area	200 m <sup>2</sup> /g
Color	White
Morphology	Nearly spherical
Density (real)	4.23 g/cm <sup>3</sup>
Density (bulk)	0.06–0.10 g/cm <sup>3</sup>

After the extraction process, all of the samples were derivatized in order to measure them easily. A derivatization procedure; 50  $\mu\text{L}$  of a mixture of BSTFA+1% TMCS and 50  $\mu\text{L}$  pyridine were used. The vials were closed and agitated for 1 min using a vortex system. Derivatization was performed at 60°C for 30 min. The derivatives were cooled to room temperature and analyzed by GC. All the pharmaceuticals were analyzed by means of a Shimadzu GC QP2010 Plus/MS and an RTX-5 column (60 m  $\times$  0.25 mm, 0.1  $\mu\text{m}$ ). The characteristic ions after the GC results were found to be similar to those obtained by Migowska et al. [15]. The retention times were 26.75 min for estrone and 30.90 min for estriol. The characteristics ions detected with GC/MS were 342,257,218  $m/z$  and 504,311,129  $m/z$  for estrone and estriol, respectively. To the best of our knowledge, these characteristic ions regarding these compounds have never been discovered before (218  $m/z$  for estrone; 129  $m/z$  for estriol). The siltation compounds formed after the derivatization of the drugs were identified with the NIST 7 library. For estrone and estriol, the compounds formed after derivatization were Estra-1,3,5 (10) trien-17-one, 3-[(trimethylsilyloxy)] and silane, [[(16a, 17a) 5 (10) -triene-3,16,17-triyl] tris (oxy)] tris [trimethyl- or tri (trimethylsilyl)] derivative of estriol. The limit of detection and limit of quantification values were 0.213 and 0.710  $\mu\text{g/L}$  for E1 and 0.195 and 0.649 for E3, respectively. In addition to these, humic acid (0–20 mg/L) and anion (0–500 mg/L) concentrations were prepared for the determination of the removal efficiency for co-existing ions.

## 3. Results and discussion

### 3.1. The characterization and the catalytic effect of catalyst

Due to its chemical stability, high photocatalytic activity and low toxicity,  $\text{TiO}_2$  is the most preferred photocatalyst for heterogeneous photocatalytic processes [16]. The photocatalyst morphology and crystallinity, presence of active groups, porosity (Brunauer–Emmett–Teller surface area) and light absorption properties are some important properties that can indicate adsorption capacity [16]. In order to identify the morphology and point of zero charge of the nanocatalyst, XRD and  $\text{pH}_{\text{pzc}}$  (batch equilibration technique) analysis was performed. The characterization analysis results are shown in Figs. 1 and 2.

According to the XRD results, the maximum peak values were  $2\theta = 25^\circ$ ,  $5^\circ$  (10–25 nm) and  $2\theta = 27^\circ$ ,  $6^\circ$  (10 nm). The high peak values showed that the material used  $\text{TiO}_2$  is anatase type as same in the literature (Fig. 1) [17,18]. The crystal structure of natural  $\text{TiO}_2$  nanoparticles appeared at  $2\theta = 25.5^\circ$ ,  $38.1^\circ$ ,  $48.1^\circ$  and  $55.2^\circ$ . These are characteristic peaks of  $\text{TiO}_2$  nanoparticles [19]. Both  $\text{TiO}_2$  particles exhibited almost identical properties. This is because the crystal structure does not change.

The initial and final values of pH were only the same at pH 7.41, thus the  $\text{pH}_{\text{pzc}}$  of  $\text{TiO}_2$  was determined as 7.41 (Fig. 2). This  $\text{pH}_{\text{pzc}}$  suggests that the surface of the catalyst should be predominantly positive at pH values lower than 7.41 and negative at pH values higher than 7.41. The surface charge density of the material should decrease when the pH of the solution approaches  $\text{pH}_{\text{pzc}}$  and increases as it deviates from  $\text{pH}_{\text{pzc}}$  [20].

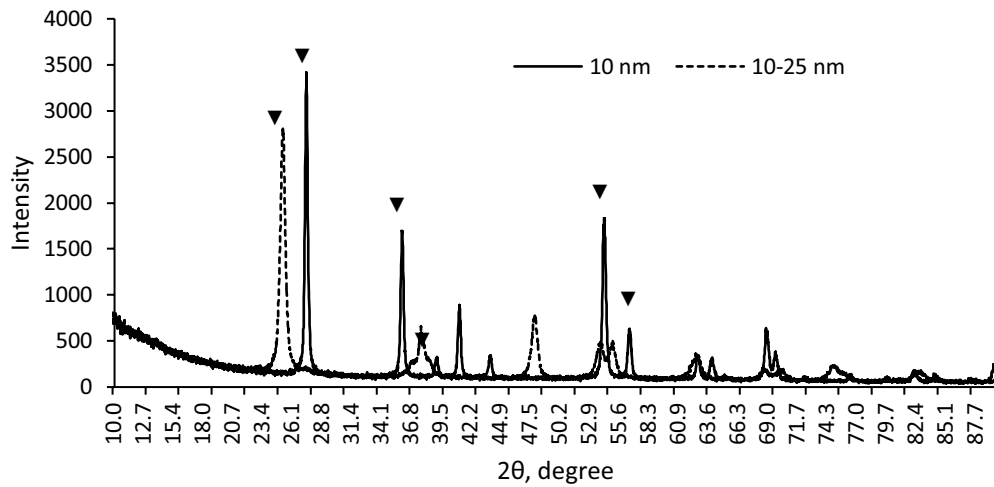


Fig. 1. The XRD graphs of nano-TiO<sub>2</sub> (▼: anatase type).

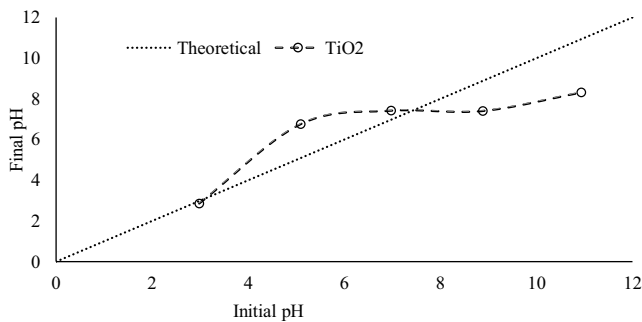


Fig. 2. The pH<sub>pzc</sub> graph of nano-TiO<sub>2</sub>.

### 3.2. Effect of catalyst dosage

As stated in the literature in the treatment of pharmaceuticals, the UV/TiO<sub>2</sub> system, which is one of the most commonly used advanced oxidation method, is used [11,21,22]. A larger specific surface area leads to increased photocatalytic activity and can also increase the potential of the recombination of electron-hole pairs as surfaces act as defects and annihilation sites [23]. In this study, the nanocomposite forms of TiO<sub>2</sub> were applied as a photocatalyst. This configuration has disadvantages such as recovery and separation from aqueous solutions during treatment [23,24]. Firstly, the effect of sole TiO<sub>2</sub> and sole UV on removal efficiency was investigated (Figs. 3–5). According to the experimental results, no effect of sole UV and sole TiO<sub>2</sub> as defined in the literature was observed [25]. In heterogeneous systems, the yield of removal is linear, with an increase in catalyst dosages [3]. In the present study, different catalyst loadings (0.025; 0.050; 0.075 and 0.1 g/L) were investigated to select a suitable loading for further experiments. It was determined that the removal efficiency increased with the increase in the amount of TiO<sub>2</sub> (Fig. 4). The greatest overall degradation of steroid hormones was observed at a catalyst dosage of 0.075 g/L for both pollutants (Fig. 6). An almost 2.04- and 3.19-fold and increases in removal efficiency was observed at UV/TiO<sub>2</sub> system, in comparison to sole UV radiation and sole TiO<sub>2</sub> for estrone

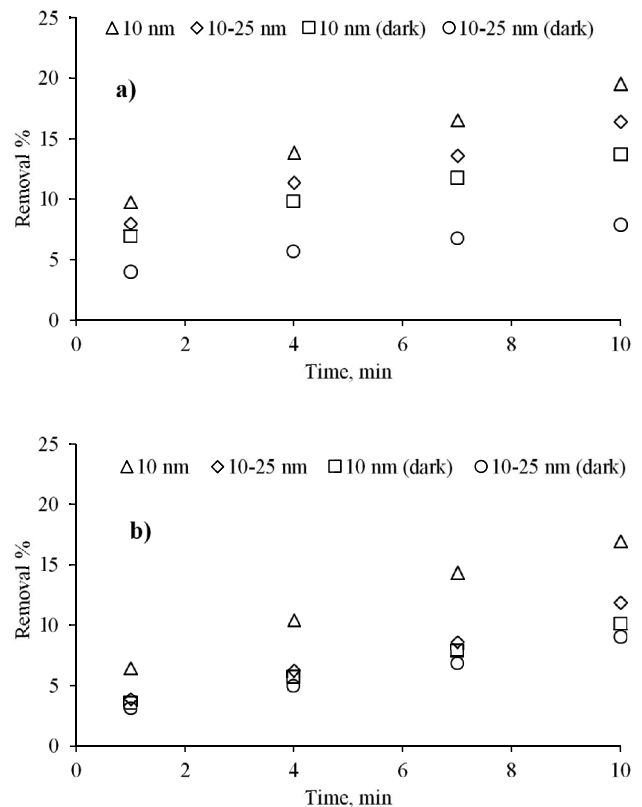


Fig. 3. Effect of sole catalyst in dark and light media in different catalyst sizes ([E1-E3] = 100 µg/L, pH = 6, 8). (a) E1 removal and (b) E3 removal.

(E1). Similarly, an almost 3.72- and 2.83-fold and decreases at removal efficiency was observed at sole UV radiation and sole TiO<sub>2</sub>, in comparison to UV/TiO<sub>2</sub> system for estriol (E3). Experimental results also showed that the smaller catalyst size provided better degradation efficiency due to the increase in the surface area (Figs. 4 and 5). It was clear that the sole UV radiation and sole TiO<sub>2</sub> was insufficient.

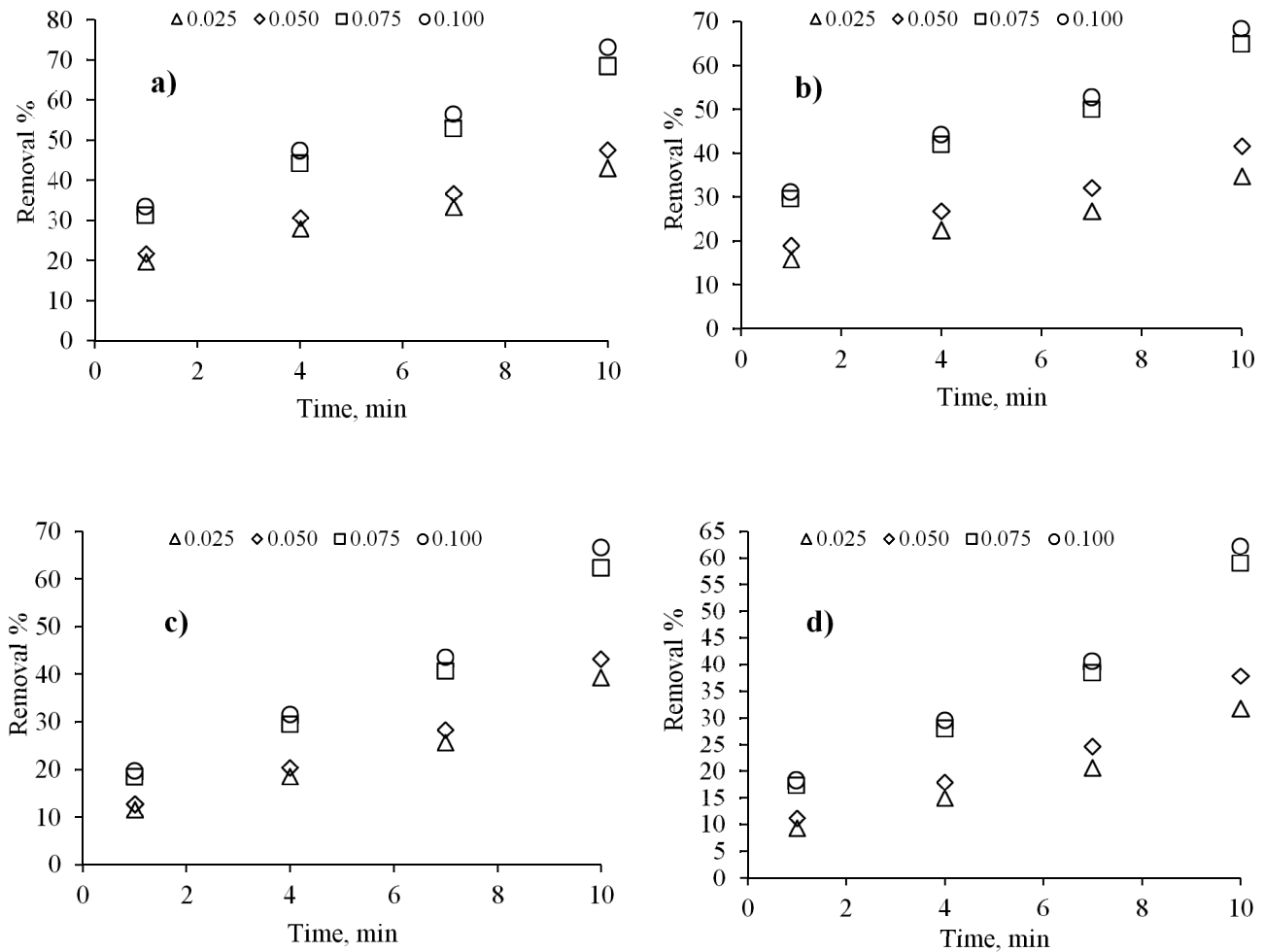


Fig. 4. Effect of catalyst dosage on removal ( $[E1-E3] = 100 \mu\text{g/L}$ ,  $\text{pH} = 6, 8$ ). (a) E1, catalyst size = 10 nm; (b) E1, catalyst size = 10–25 nm; (c) E3, catalyst size = 10 nm; (d) E3, catalyst size = 10–25 nm.

However, the photocatalytic system was feasible and the smaller size was feasible for degradation.

### 3.3. pH effect

pH value is one of the most important parameters in heterogeneous photocatalytic systems. The pH value significantly affects the precipitation of the catalyst, the charge of the  $\text{TiO}_2$  surface and the ionization state of the organic molecules [26]. In order to explain the behavior of target estrogens under different pH conditions, the mechanism of photocatalytic purification must be understood. This mechanism includes (i) adsorption and (ii) the reaction between hydroxyl radicals and holes that occur on the catalyst surface. pH depends on the  $\text{TiO}_2$  charge and estrogen ionization degree at different pH values. The  $\text{TiO}_2$  surface is amphoteric, thus, different charged species occur in different pH conditions. The  $\text{pH}_{\text{pzc}}$  value is a good indication of surface load conditions at different pH values. Hence, the charge of  $\text{TiO}_2$  was positive at acidic media and negative in basic media ( $\text{pH}_{\text{pzc}}$  value of  $\text{TiO}_2 = 7.41$ ). The surface charge was negative, positive

and neutral, when  $\text{pH} > \text{pH}_{\text{pzc}}$ ,  $\text{pH} < \text{pH}_{\text{pzc}}$  and  $\text{pH} = \text{pH}_{\text{pzc}}$  respectively. According to their  $\text{pK}_a$  values, the steroid hormones, namely E1 and E3, were neutral in acidic conditions and negative in basic conditions [12]. Under basic conditions, electrostatic repulsion occurs between the negatively charged  $\text{TiO}_2$  surface and the target compounds. As a result, the oxidation of organic molecules by different species related to  $\text{TiO}_2$  photocatalysis is reduced [27]. It is much easier to observe the interaction between charged compounds and the  $\text{TiO}_2$  surface, the interaction of the neutral compounds is related to the pH value of the solution and the potential for electron acceptance (nucleophilicity) of these compounds. The neutral compound is adsorbed to the charged  $\text{TiO}_2$  surface if it is in a more electron accepting capacity (more powerful nucleophile) and the pH of the solution is close to the  $\text{pH}_{\text{pzc}}$  value [28]. Many organic compounds form ionic bonds with metal oxides such as  $\text{TiO}_2$  [29]. As a result, the oxidation of neutral pollutants such as the target compounds in this study can be achieved by the  $\text{TiO}_2$  photocatalytic system. In the present study, target estrogenic compound removal was feasible at neutral conditions rather than negative conditions (Fig. 6).

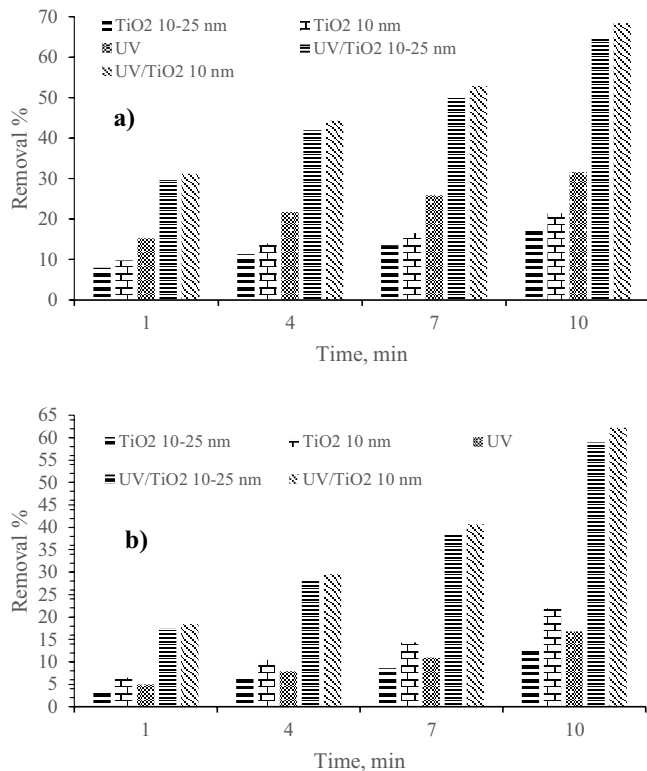


Fig. 5. Removal of steroids hormones with different systems ( $[E1-E3] = 100 \mu\text{g/L}$ ,  $\text{pH} = 6, 8$ ). (a) E1 removal and (b) E3 removal.

The pH effect on the removal of the target estrogens was investigated with pH values of 3 (acidic), 6.8 (neutral) and 10 (basic). When pH increased from 3 to 6.8, the removal efficiencies of E1 and E3 decreased from 71.85% and 68.43% to 71.54% and 62.21%, respectively. When pH further increased to 10, the removal efficiencies of E1 and E3 only decreased to 48.59% and 44.17%, respectively. The optimum pH was selected as 6.8 (neutral) because of no pH adjustment. Moreover, as stated in the literature, due to the fact that the molecular structures of the synthetic hormones (E1-E3) used in this study were similar, a similar effect was observed in the removal mechanism [12]. In addition, it can be concluded from Table 2 that estrogen (EDC) removal by UV/TiO<sub>2</sub> photocatalytic oxidation was an efficient method compared to various removal efficiencies and operation times reported in similar studies in the literature.

Table 2  
EDC removal efficiencies with various methods (%)

EDC	Process	Removal efficiency %	Time (min)	Sources
E1-E3	UVC/TiO <sub>2</sub>	98–60	180	[30]
E1-E3	UVA/TiO <sub>2</sub>	49–20	180	[30]
E1-E3	UV LED/porous TiO <sub>2</sub>	~100	120	[12]
E1-E3	UV/immobilized TiO <sub>2</sub>	95–95	100	[31]
E1	UV/TiO <sub>2</sub> P25	95	10	[9]
E1	UV/TiO <sub>2</sub> -S21 Sigma-Aldrich	80	260	[32]
E1-E3	UV/nano-TiO <sub>2</sub> (different particle size)	65–57	10	This study

### 3.4. Kinetic study

The Langmuir–Hinshelwood (L–H) mechanism is used to describe the photocatalytic oxidation kinetics [12,30]. When TiO<sub>2</sub> was used as the catalyst, the photocatalytic kinetics of organic compounds conformed to the L–H model principle, which describes reactions between radicals and molecules [30,31]. Langmuir–Hinshelwood kinetic model is given in the following equation [32]:

$$r = -\frac{dC}{dt} = \frac{CKkr}{1+KC} \quad (1)$$

where  $r$  is the rate of degradation,  $K$  is the equilibrium constant for the adsorption of organic molecules on the catalyst surface and  $kr$  is the reaction constant. This equation can also be written in the following form (Eq. (2)):

$$\frac{\ln C_0}{C} \approx krKt = k't \quad (2)$$

Eq. (2) can only be utilized if the initial pollutant concentration is very low [33]. The obtained constant rates of removal at photocatalytic are shown in Tables 3 and 4.

### 3.5. Effect of humic acid and anion concentrations on removal efficiency

Due to the photosensitizing ability, increasing humic acid concentrations at stable level (5–15 mg/L), the degradation efficiency is also increased (Fig. 7). After 20 mg/L, the removal efficiency decreased as the reaction between humic acid and active radicals and the turbidity effect. Similar results regarding the same effect of humic acid were reported in various studies in the literature [34,35].

Anion concentration varying from 0 to 500 mg/L was tested for finding on removal efficiency of target pollutants (Fig. 8). It was determined that sulfate, chloride and nitrate concentration had an insignificant effect on removal efficiency. As similar as literature, these radicals will affect the reaction between pollutants and radicals [36]. By increasing the bicarbonate, carbonate and phosphate concentrations from 0 to 500 mg/L, the removal efficiency was rendered because of the hydroxyl radical scavenging properties and consumption of holes by high anion concentrations.

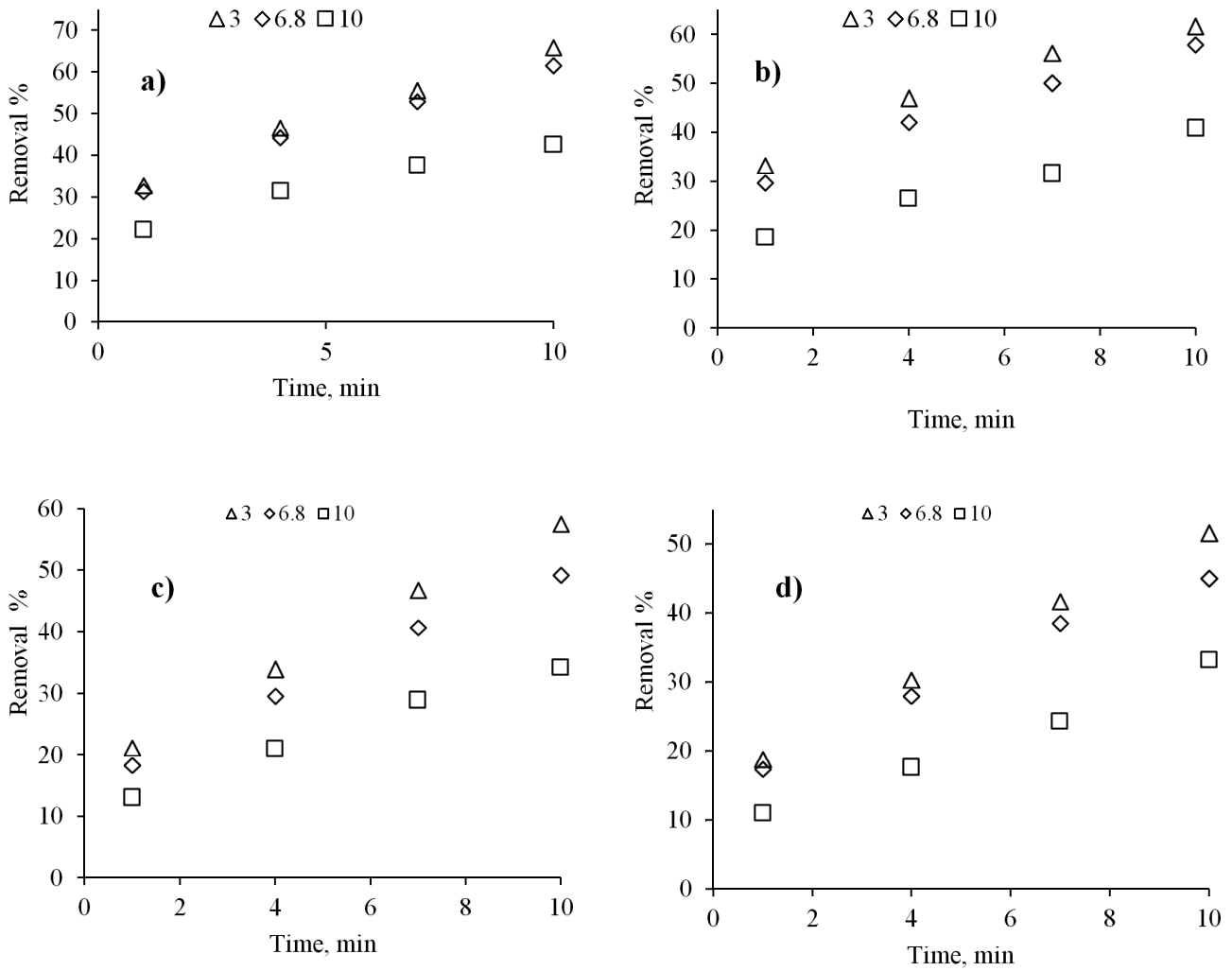


Fig. 6. Effect of pH on removal ([E1-E3] = 100  $\mu\text{g/L}$ , catalyst dosage = 0.075 g/L). (a) E1, catalyst size = 10 nm; (b) E1, catalyst size = 10–25 nm; (c) E3, catalyst size = 10 nm; (d) E3, catalyst size = 10–25 nm.

Table 3

The coefficients of characteristic constants of the kinetic model (all experimental studies) (E1 compound)

			0.025	0.05	0.075	0.1	
Catalyst size (10 nm)	Catalyst dosage (g/L)	<i>k</i>	0.0372	0.0432	0.0834	0.0974	
		<i>R</i> <sup>2</sup>	0.9798	0.9777	0.9603	0.9530	
	pH and sole catalyst			3	6.8	10	Sole catalyst
		<i>k</i>		0.0932	0.0834	0.0446	0.0149
		<i>R</i> <sup>2</sup>		0.9552	0.9603	0.9772	0.9860
				0.025	0.05	0.075	0.1
Catalyst size (10–25 nm)	Catalyst dosage (g/L)	<i>k</i>	0.0275	0.0353	0.0745	0.0832	
		<i>R</i> <sup>2</sup>	0.9827	0.9804	0.9646	0.9604	
	pH and sole catalyst			3	6.8	10	Sole catalyst
		<i>k</i>		0.0956	0.0745	0.0343	0.0118
		<i>R</i> <sup>2</sup>		0.9539	0.9646	0.9807	0.9866
				0.025	0.05	0.075	0.1

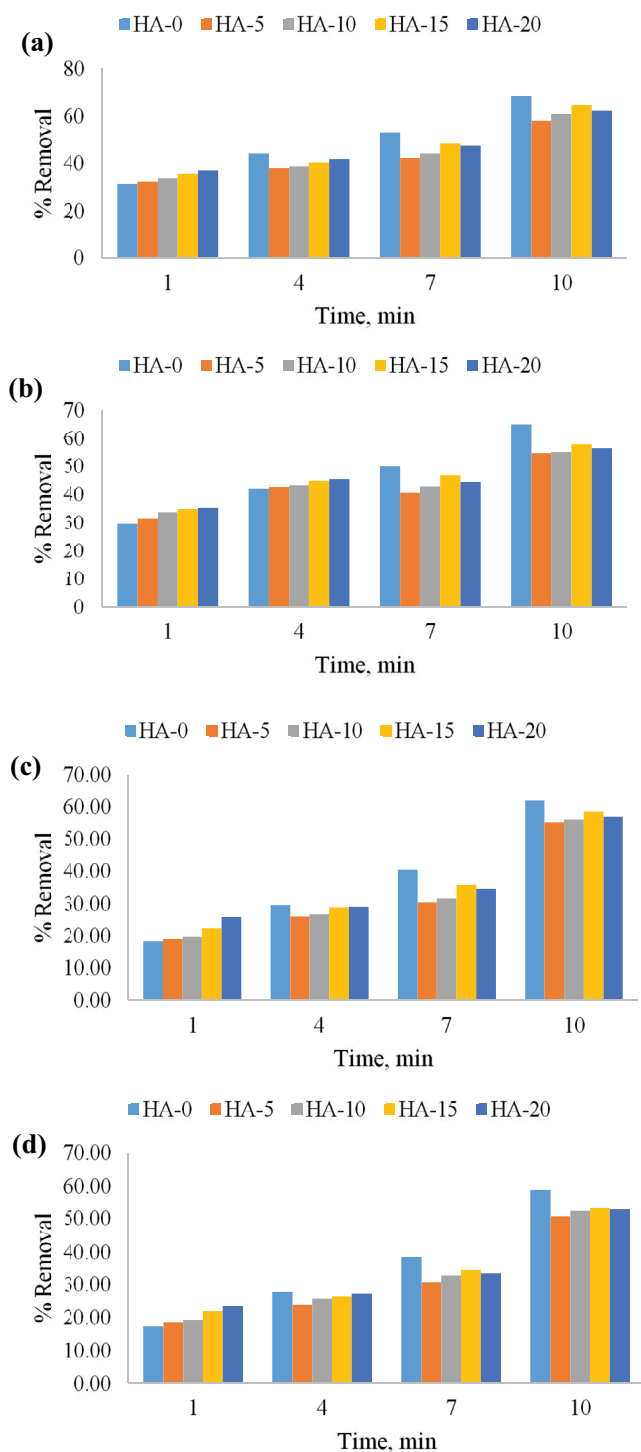


Fig. 7. Effect of humic acid on removal of pollutants ( $[E1-E3] = 100 \mu\text{g/L}$ , catalyst dosage =  $0.075 \text{ g/L}$ ,  $\text{pH} = 6, 8$ . (a) E1, catalyst size =  $10 \text{ nm}$ ; (b) E1, catalyst size =  $10-25 \text{ nm}$ ; (c) E3, catalyst size =  $10 \text{ nm}$ ; (d) E3, catalyst size =  $10-25 \text{ nm}$ ).

#### 4. Conclusion

In this study, nano-TiO<sub>2</sub> was used and the steroid hormone removal ability from the photocatalytic reactor with a low-pressure lamp was investigated.

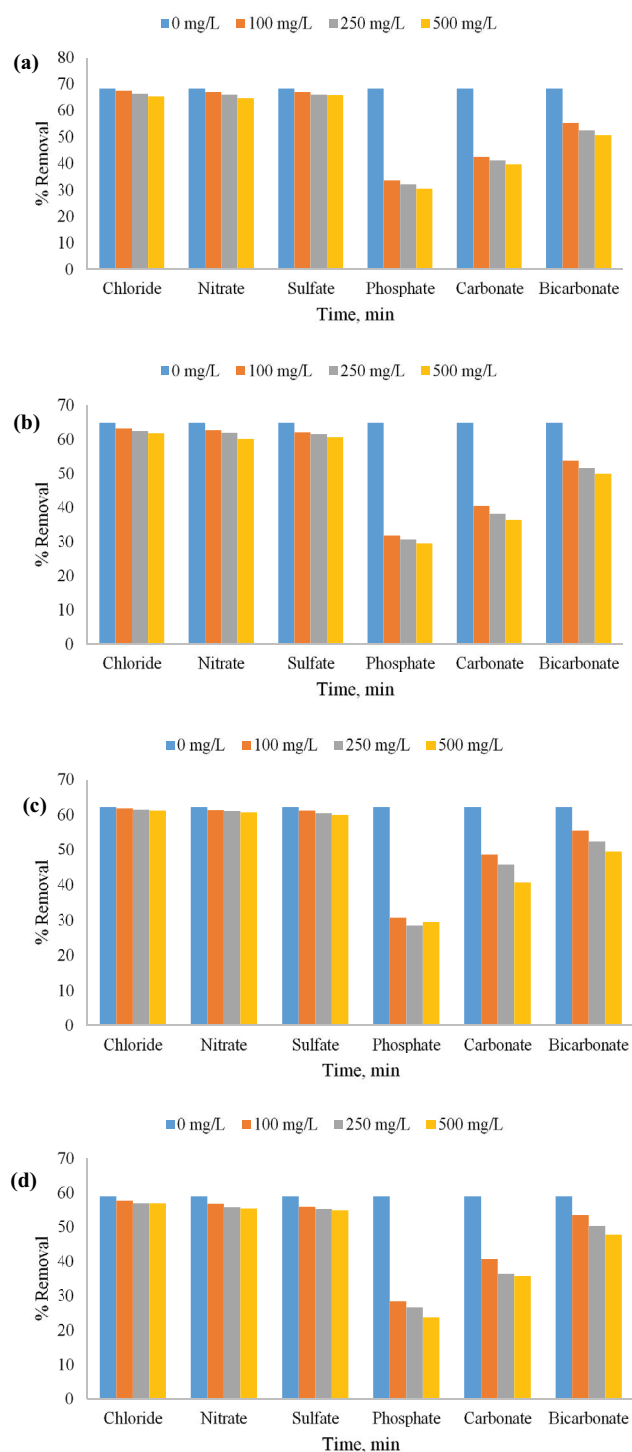


Fig. 8. Effect of anions on removal of target pollutants ( $[E1-E3] = 100 \mu\text{g/L}$ , catalyst dosage =  $0.075 \text{ g/L}$ ,  $\text{pH} = 6, 8$ . (a) E1, catalyst size =  $10 \text{ nm}$ ; (b) E1, catalyst size =  $10-25 \text{ nm}$ ; (c) E3, catalyst size =  $10 \text{ nm}$ ; (d) E3, catalyst size =  $10-25 \text{ nm}$ ).

It was observed that the presence of nano-TiO<sub>2</sub> enhanced the photodegradation of E1 and E3 and that particle size was an important factor influencing degradation efficiency. Comparing the performance of the different sized catalysts, it can be concluded that the high surface area

Table 4

The coefficients of characteristic constants of the kinetic model (all experimental studies) (E3 compound)

			0.025	0.05	0.075	0.1
Catalyst size (10 nm)	Catalyst dosage (g/L)	<i>k</i>	0.0405	0.0465	0.0828	0.0940
		<i>R</i> <sup>2</sup>	0.9475	0.9440	0.9210	0.9135
	pH and sole catalyst	<i>k</i>	0.0828	0.1091	0.0478	0.0196
		<i>R</i> <sup>2</sup>	0.9210	0.9032	0.9432	0.9592
Catalyst size (10–25 nm)	Catalyst dosage (g/L)	<i>k</i>	0.0306	0.0387	0.0752	0.0826
		<i>R</i> <sup>2</sup>	0.9532	0.9486	0.9260	0.9211
	pH and sole catalyst	<i>k</i>	0.0752	0.0864	0.0376	0.0110
		<i>R</i> <sup>2</sup>	0.9260	0.9186	0.9492	0.9636

of nano-TiO<sub>2</sub> enhances the removal efficiency and that the smaller catalyst surface in particular showed a better removal efficiency of the selected pollutants.

Moreover, the optimum condition of the process was achieved at a catalyst dosage of 0.075 g/L and a pH of 6.8. When the results are observed, it can be concluded that the use of the Response Surface Methodology approach can be useful for the degradation and a more effective method belong to short irradiation time. The effect of humic acid concentration was also investigated and it was determined that an increase in humic acid concentration at a certain level, increased the removal efficiency. Various coexisting anions such as sulfate, chloride and nitrate, did not affect the removal efficiency. However, some anions including bicarbonate, carbonate and phosphate decreased the removal efficiency due to their hydroxyl scavenging properties. The kinetic data revealed that the decolorization was fitted by Langmuir–Hinshelwood model. Due to the synergic effect of adsorption, the photocatalytic degradation efficiency of the pollutants can increase.

### Acknowledgments

This work was funded by the Scientific and Technological Research Council of Turkey (2211 C program) and supported by the Scientific Research Projects Coordinatorship of Aksaray University (2014-028 and 2015-057 project). The authors would like to thank Dr. Alper ALVER for his valuable comments and helpful revision suggestions.

### Conflict of interest

There is no conflict of interest between the authors.

### References

- [1] A.R. Ribeiro, O.C. Nunes, M.F. Pereira, A.M. Silva, An overview on the advanced oxidation processes applied for the treatment of water pollutants defined in the recently launched Directive 2013/39/EU, *Environ. Int.*, 75 (2015) 33–51.
- [2] M.O. Barbosa, N.F. Moreira, A.R. Ribeiro, M.F. Pereira, A.M. Silva, Occurrence and removal of organic micropollutants: an overview of the watch list of EU Decision 2015/495, *Water Res.*, 94 (2016) 257–279.
- [3] Z. Pan, E.A. Stemmler, H.J. Cho, W. Fan, L.A. LeBlanc, H.H. Patterson, A. Amirbahman, Photocatalytic degradation of 17 $\alpha$ -ethinylestradiol (EE2) in the presence of TiO<sub>2</sub>-doped zeolite, *J. Hazard. Mater.*, 279 (2014) 17–25.
- [4] S. Sarkar, S. Ali, L. Rehmman, G. Nakhla, M.B. Ray, Degradation of estrone in water and wastewater by various advanced oxidation processes, *J. Hazard. Mater.*, 278 (2014) 16–24.
- [5] J.C. Carlson, M.I. Stefan, J.M. Parnis, C.D. Metcalfe, Direct UV photolysis of selected pharmaceuticals, personal care products and endocrine disruptors in aqueous solution, *Water Res.*, 84 (2015) 350–361.
- [6] Y. Li, A. Zhang, Removal of steroid estrogens from waste activated sludge using Fenton oxidation: Influencing factors and degradation intermediates, *Chemosphere*, 105 (2014) 24–30.
- [7] Y. Lin, Z. Peng, X. Zhang, Ozonation of estrone, estradiol, diethylstilbestrol in waters, *Desalination*, 249 (2009) 235–240.
- [8] K. Sornalingam, A. McDonagh, J.L. Zhou, M.A.H. Johir, M.B. Ahmed, Photocatalysis of estrone in water and wastewater: comparison between Au-TiO<sub>2</sub> nanocomposite and TiO<sub>2</sub> and degradation by-products, *Sci. Total Environ.*, 610 (2018) 521–530.
- [9] J. Han, Y. Liu, N. Singhal, L. Wang, W. Gao, Comparative photocatalytic degradation of estrone in water by ZnO and TiO<sub>2</sub> under artificial UVA and solar irradiation, *Chem. Eng. J.*, 213 (2012) 150–162.
- [10] Y. Souissi, S. Bourcier, S. Bouchonnet, C. Genty, M. Sablier, Estrone direct photolysis: by-product identification using LC-Q-TOF, *Chemosphere*, 87 (2012) 185–193.
- [11] M.R. Eskandarian, H. Choi, M. Fazli, M.H. Rasoulifard, Effect of UV-LED wavelengths on direct photolytic and TiO<sub>2</sub> photocatalytic degradation of emerging contaminants in water, *Chem. Eng. J.*, 300 (2016) 414–422.
- [12] M.J. Arlos, R. Liang, M.M. Hatat-Fraile, L.M. Bragg, N.Y. Zhou, M.R. Servos, S.A. Andrews, Photocatalytic decomposition of selected estrogens and their estrogenic activity by UV-LED irradiated TiO<sub>2</sub> immobilized on porous titanium sheets via thermal-chemical oxidation, *J. Hazard. Mater.*, 318 (2016) 541–550.
- [13] M.J. Arlos, M.M. Hatat-Fraile, R. Liang, L.M. Bragg, N.Y. Zhou, S.A. Andrews, M.R. Servos, Photocatalytic decomposition of organic micropollutants using immobilized TiO<sub>2</sub> having different isoelectric points, *Water Res.*, 101 (2016) 351–361.
- [14] Y. Huang, C. Cui, D. Zhang, L. Li, D. Pan, Heterogeneous catalytic ozonation of dibutyl phthalate in aqueous solution in the presence of iron-loaded activated carbon, *Chemosphere*, 119 (2015) 295–301.



- [15] N. Migowska, M. Caban, P. Stepnowski, J. Kumirska, Simultaneous analysis of non-steroidal anti-inflammatory drugs and estrogenic hormones in water and wastewater samples using gas chromatography–mass spectrometry and gas chromatography with electron capture detection, *Sci. Total Environ.*, 441 (2012) 77–88.
- [16] M. Mehrjouei, S. Müller, D. Möller, A review on photocatalytic ozonation used for the treatment of water and wastewater, *Chem. Eng. J.*, 263 (2015) 209–219.
- [17] G. Liao, D. Zhu, J. Zheng, J. Yin, B. Lan, L. Li, Efficient mineralization of bisphenol A by photocatalytic ozonation with TiO<sub>2</sub>–graphene hybrid, *J. Taiwan Inst. Chem. Eng.*, 67 (2016) 300–305.
- [18] J. Bing, C. Hu, L. Zhang, Enhanced mineralization of pharmaceuticals by surface oxidation over mesoporous  $\gamma$ -Ti-AlO<sub>3</sub> suspension with ozone, *Appl. Catal., B*, 202 (2017) 118–126.
- [19] K. Thamaphat, P. Limsuwan, B. Ngotawornchai, Phase characterization of TiO<sub>2</sub> powder by XRD and TEM, *Kasetsart J. (Nat. Sci.)*, 42 (2008) 357–361.
- [20] P. Nuengmacha, S. Chanthai, R. Mahachai, W.-C. Oh, Sonocatalytic performance of ZnO/graphene/TiO<sub>2</sub> nanocomposite for degradation of dye pollutants (methylene blue, texbrite BAC-L, texbrite BBU-L and texbrite NFW-L) under ultrasonic irradiation, *Dyes Pigm.*, 134 (2016) 487–497.
- [21] R.L. Fernández, J.A. McDonald, S.J. Khan, P. Le-Clech, Removal of pharmaceuticals and endocrine disrupting chemicals by a submerged membrane photocatalysis reactor (MPR), *Sep. Purif. Technol.*, 127 (2014) 131–139.
- [22] R. Szabó, C. Megyeri, E. Illés, K. Gajda-Schranz, P. Mazellier, A. Dombi, Phototransformation of ibuprofen and ketoprofen in aqueous solutions, *Chemosphere*, 84 (2011) 1658–1663.
- [23] G. Varshney, S.R. Kanel, D.M. Kempisty, V. Varshney, A. Agrawal, E. Sahle-Demessie, R.S. Varma, M.N. Nadagouda, Nanoscale TiO<sub>2</sub> films and their application in remediation of organic pollutants, *Coord. Chem. Rev.*, 306 (2016) 43–64.
- [24] Z. Clemente, V. Castro, C. Jonsson, L. Fraceto, Ecotoxicology of nano-TiO<sub>2</sub>—an evaluation of its toxicity to organisms of aquatic ecosystems, *Int. J. Environ. Res.*, 6 (2011) 33–50.
- [25] X. Van Doorslaer, K. Demeestere, P.M. Heynderickx, H. Van Langenhove, J. Dewulf, UV-A and UV-C induced photolytic and photocatalytic degradation of aqueous ciprofloxacin and moxifloxacin: reaction kinetics and role of adsorption, *Appl. Catal., B*, 101 (2011) 540–547.
- [26] J.I. Sobral Romao, *Photocatalytic Water Treatment: Substrate-Specific Activity of Titanium Dioxide*, Faculty of Science and Technology, Universiteit Twente, 2015.
- [27] M. Lu, P. Pichat, *Photocatalysis and Water Purification: From Fundamentals to Recent Applications*, John Wiley & Sons, Weinheim, 2013.
- [28] A. Rodríguez, R. Rosal, J. Perdigón-Melón, M. Mezcua, A. Agüera, M. Hernando, P. Letón, A. Fernández-Alba, E. García-Calvo, *Ozone-based Technologies in Water and Wastewater Treatment*, In: *The Handbook of Environmental Chemistry*, Springer, Berlin, Heidelberg, 2008.
- [29] W.Z. Tang, *Physicochemical Treatment of Hazardous Wastes*, CRC Press, 2016.
- [30] I.K. Konstantinou, T.A. Albanis, TiO<sub>2</sub>-assisted photocatalytic degradation of azo dyes in aqueous solution: kinetic and mechanistic investigations: a review, *Appl. Catal., B*, 49 (2004) 1–14.
- [31] T.E. Doll, F.H. Frimmel, Kinetic study of photocatalytic degradation of carbamazepine, clofibric acid, iomeprol and iopromide assisted by different TiO<sub>2</sub> materials—determination of intermediates and reaction pathways, *Water Res.*, 38 (2004) 955–964.
- [32] H.B. Hadjiltaief, M.B. Zina, M.E. Galvez, P. Da Costa, Photocatalytic degradation of methyl green dye in aqueous solution over natural clay-supported ZnO–TiO<sub>2</sub> catalysts, *J. Photochem. Photobiol., A*, 315 (2016) 25–33.
- [33] Y. He, N.B. Sutton, H.H. Rijnaarts, A.A. Langenhoff, Degradation of pharmaceuticals in wastewater using immobilized TiO<sub>2</sub> photocatalysis under simulated solar irradiation, *Appl. Catal., B*, 182 (2016) 132–141.
- [34] J. Porras, C. Bedoya, J. Silva-Agredo, A. Santamaría, J.J. Fernández, R.A. Torres-Palma, Role of humic substances in the degradation pathways and residual antibacterial activity during the photodecomposition of the antibiotic ciprofloxacin in water, *Water Res.*, 94 (2016) 1–9.
- [35] F. Wang, Y. Feng, P. Chen, Y. Wang, Y. Su, Q. Zhang, Y. Zeng, Z. Xie, H. Liu, Y. Liu, Photocatalytic degradation of fluoroquinolone antibiotics using ordered mesoporous g-C<sub>3</sub>N<sub>4</sub> under simulated sunlight irradiation: kinetics, mechanism, and antibacterial activity elimination, *Appl. Catal., B*, 227 (2018) 114–122.
- [36] M. Chen, J. Yao, Y. Huang, H. Gong, W. Chu, Enhanced photocatalytic degradation of ciprofloxacin over Bi<sub>2</sub>O<sub>3</sub>/(BiO)<sub>2</sub>CO<sub>3</sub> heterojunctions: efficiency, kinetics, pathways, mechanisms and toxicity evaluation, *Chem. Eng. J.*, 334 (2018) 453–461.